

Supporting Information

Water-soluble Dinuclear Iridium(III) and Ruthenium(II) Bis-terdentate Complexes: Photophysics and Electrochemiluminescence

Bingqing Liu,^a Xin Yang,^b Mahammed Jabed,^a Svetlana Kilina,^a Zhengchun Yang,^{*,b} Wenfang Sun^{*,a}

^a Department of Chemistry and Biochemistry, North Dakota State University, Fargo, ND 58108-6050, USA

^b School of Integrated Circuit Science and Engineering, Tianjin University of Technology, Tianjin 300384, P. R. China

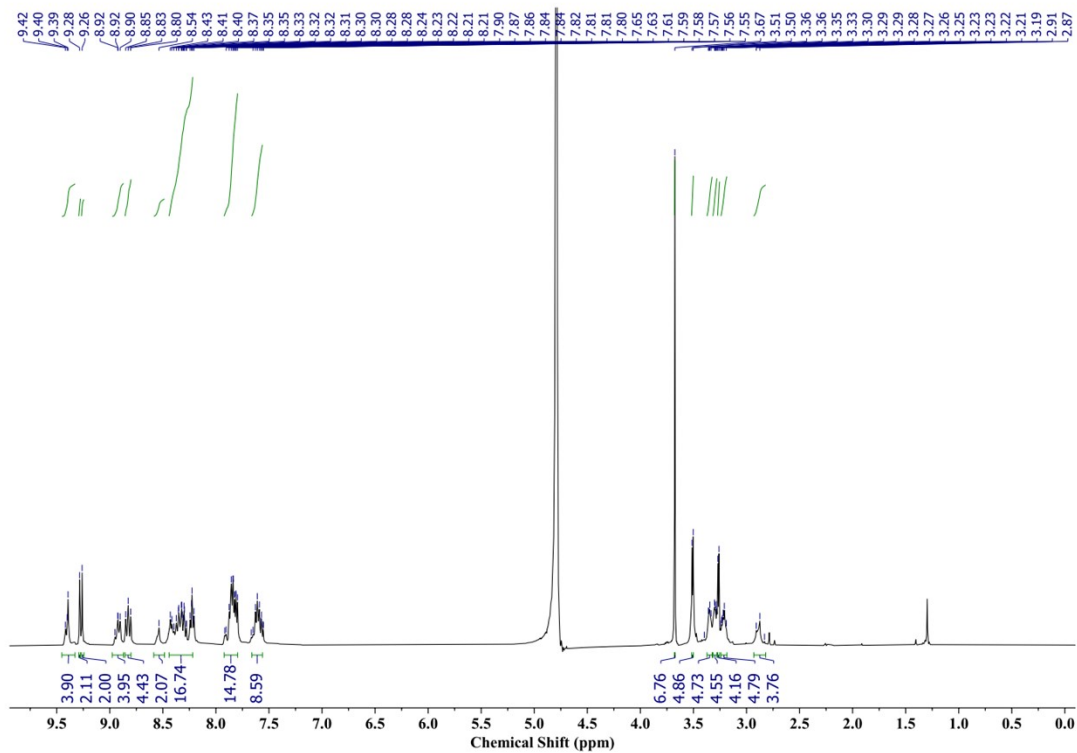


Figure S1. ^1H NMR spectrum of complex **1** in D_2O (400 MHz).

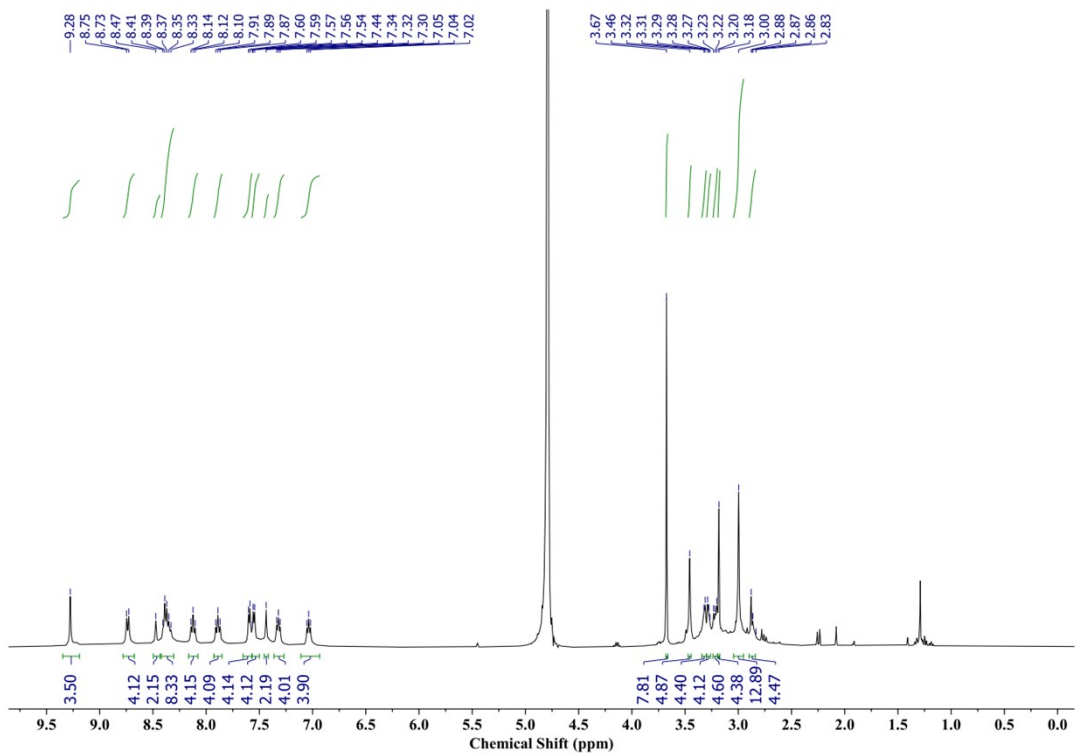


Figure S2. ^1H NMR spectrum of **2** in D_2O (400 MHz).

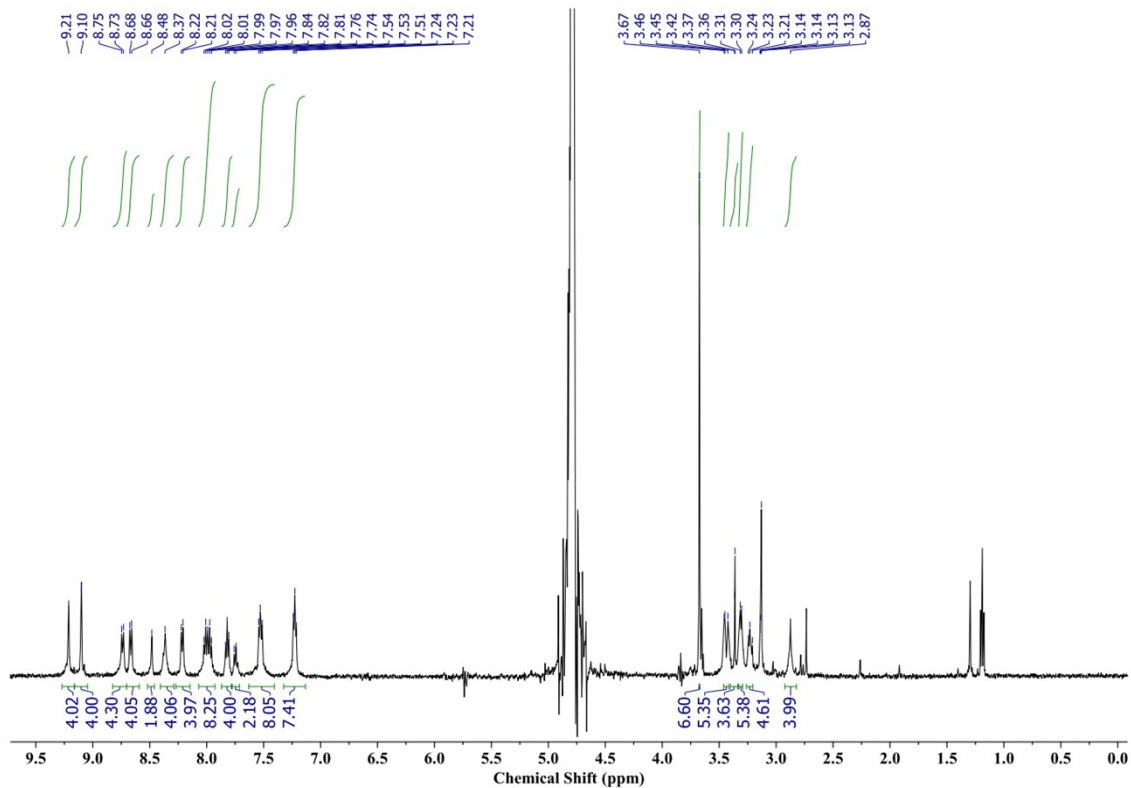


Figure S3. ^1H NMR spectrum of **3** in D_2O (500 MHz).

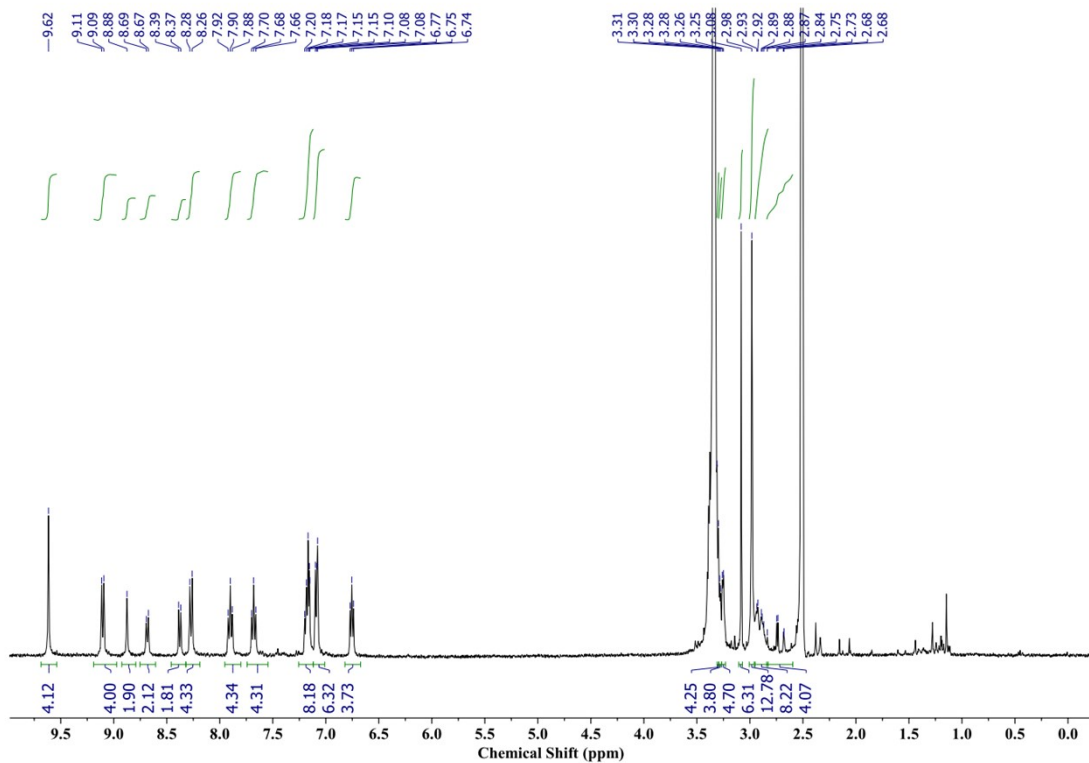


Figure S4. ^1H NMR spectrum of **4** in $\text{DMSO}-d_6$ (400 MHz).

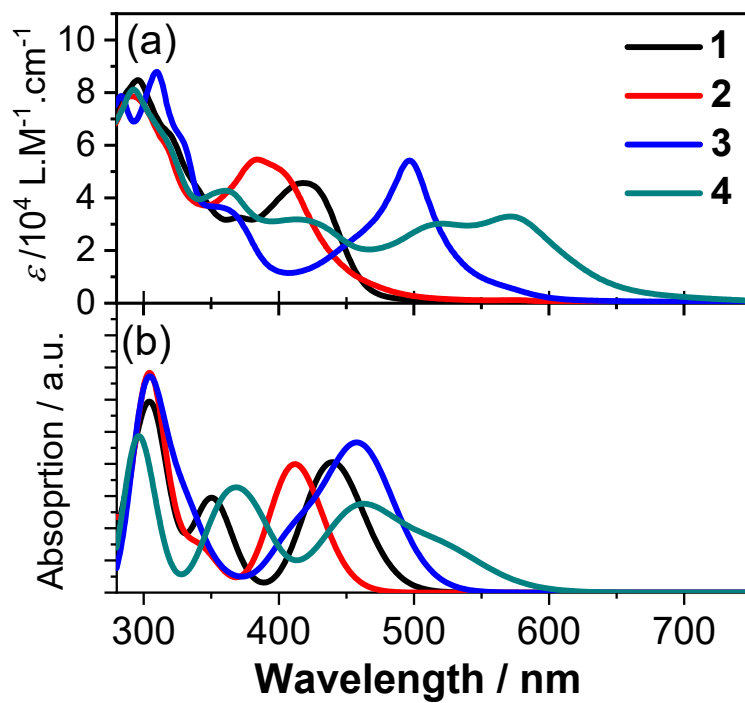


Fig. S5. (a) Experimental and (b) calculated absorption spectra of **1-4** in water. The two Ir(III) complexes **1** and **2** were calculated using PBE0 and the two Ru(II) complexes **3** and **4** were calculated using the B3LYP functional.

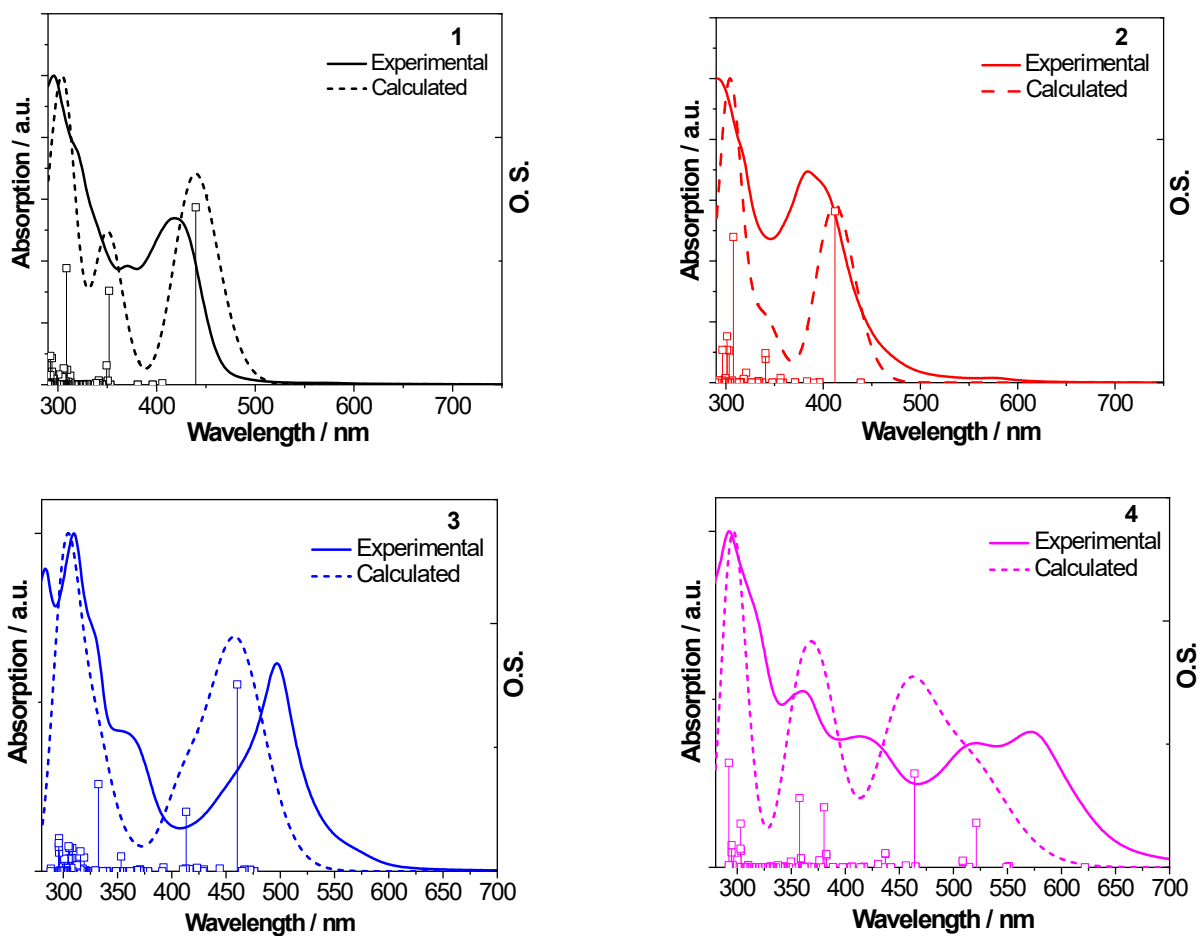


Fig. S6. Comparison of the normalized experimental and calculated absorption spectra for complexes **1-4** in water. **1** and **2** were calculated using the PBE0 functional and complexes **3** and **4** were calculated using the B3LYP functional.

Table S1. Natural transition orbitals of the high-energy transitions for complex **1**. The TDDFT calculations were conducted using PBE0 functional, LAN2dz/6-31G* basis set, and water as solvent.

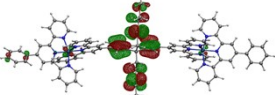

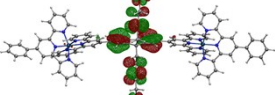
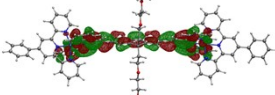
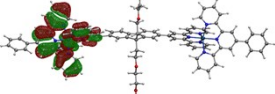
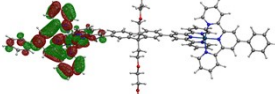
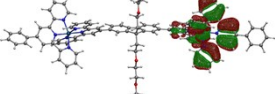
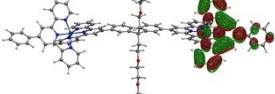
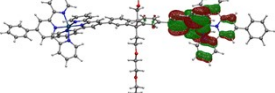
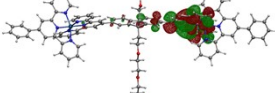
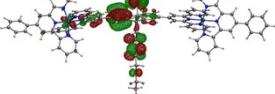
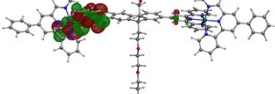
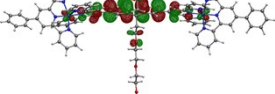
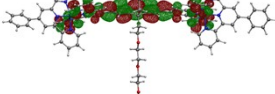
S_n and Properties	Hole	Electron
S_9 352 nm $f = 0.759$		
S_{11} 349 nm $f = 0.156$		
S_{14} 342 nm $f = 0.022$		
S_{15} 342 nm $f = 0.027$		
S_{16} 341 nm $f = 0.035$		
S_{41} 313 nm $f = 0.023$		
S_{49} 309 nm $f = 0.942$		

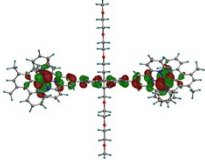
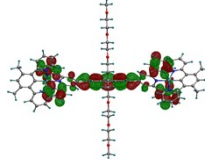
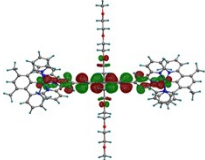
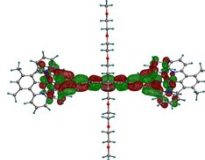
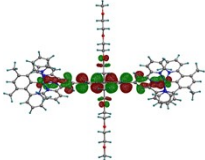
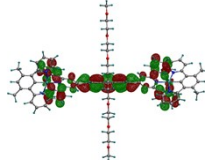
Table S2. Natural transition orbitals of the high-energy transitions for complex **2**. The TDDFT calculations were conducted using PBE0 functional, LAN2dz/6-31G* basis set, and water as solvent.

	Hole	Electron
S ₁₇ 341 nm $f = 0.194$		
S ₁₈ 341 nm $F = 0.243$		
S ₃₆ 308 nm $f = 1.199$		
S ₄₀ 303 nm $f = 0.263$		

Table S3. Natural transition orbitals of the high-energy transitions for complex **3**. The TDDFT calculations were conducted using B3LYP functional, LAN2dz/6-31G* basis set, and water as solvent.

	Hole	Electron
S ₄₁ 353 nm $f = 0.119$		
S ₅₅ 332 nm $f = 0.704$		
S ₁₁₅ 296 nm $f = 0.266$		

Table S4. Natural transition orbitals of the high-energy transitions for complex 4. The TDDFT calculations were conducted using B3LYP functional, LAN2dz/6-31G* basis set, and water as solvent.

	Hole	Electron
S_{39} 380 nm $f = 0.488$		
S_{53} 358 nm $f = 0.563$		
S_{129} 292 nm $f = 0.849$		

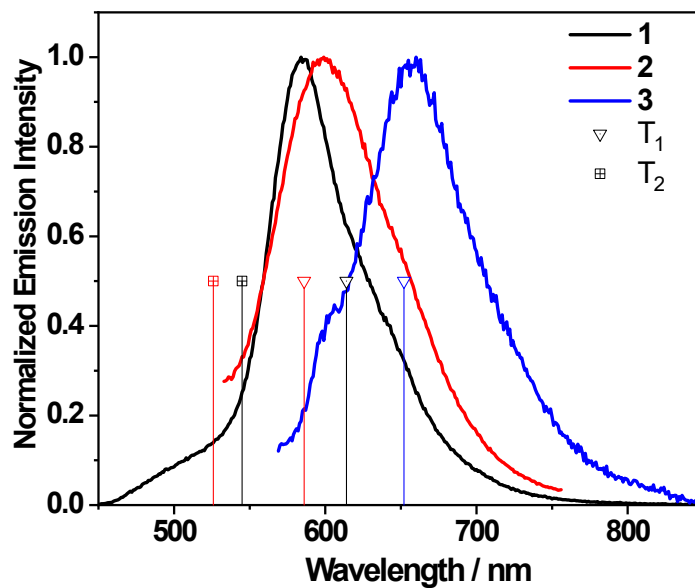


Fig. S7. Experimental emission spectra and calculated emission energies for complexes **1-3** in water. Emission energies are calculated by optimizing the triplet state (T_1) using analytical TDDFT method, the PBE0 functional, LAN2DZ/6-31G* basis sets and CPCM solvation method with water being used as a solvent. Bar heights are chosen randomly for a better representation.

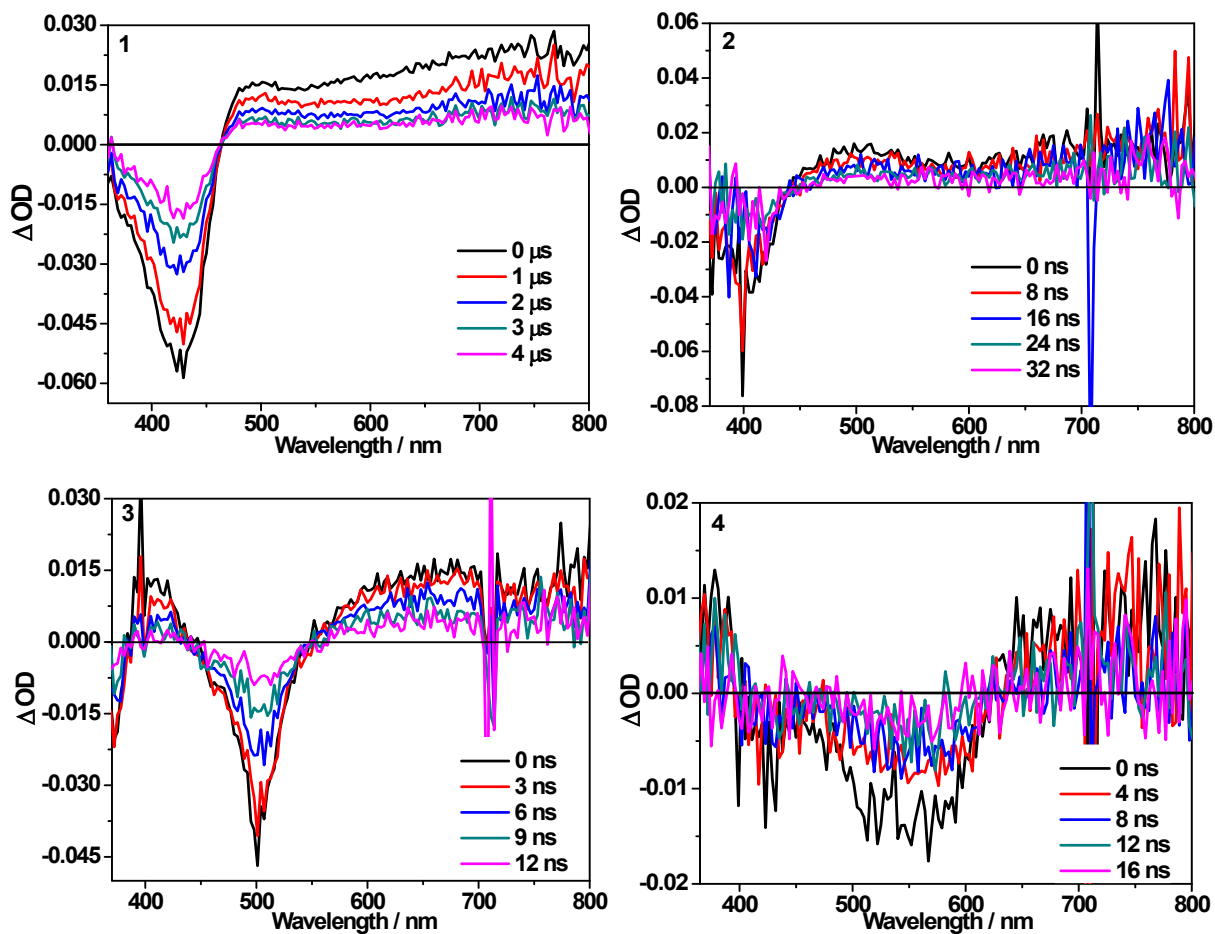


Fig. S8. Time-resolved ns-TA spectra of complexes 1–4 in acetonitrile at room temperature after 355 nm laser excitation. $A_{355} = 0.4$ in a 1 cm cuvette.